

Density functional theory approach towards bioactivity analysis of Isovallesiachotamine natural bio molecule

Ashok Kumar Mishra^{1*} and Satya Prakash Tewari²

^{1,2} Department of Physics, Dr. Shakuntala Misra National Rehabilitation University, Lucknow, India-226017

*Corresponding Author: akmishra2k5@gmail.com

Available online at: www.isroset.org

Received: 25/Mar/2019, Accepted: 19/Apr/2019, Online: 30/Apr/2019

Abstract— Present investigation focuses on the analysis of the bioactivity contained in plant-derived natural bio molecule namely Iso-vallesiachotamine using density functional theory. In this view its Infra-Red active vibrations, Raman scattering activity, UV-visible absorption, ¹H & ¹³C NMR chemical shifts, zero-point vibrational energy, enthalpy, molar heat capacity at constant volume, entropy, dipole moment, polarizability, first order hyperpolarizability and chemical reactivity have been evaluated at its optimized geometry using DFT-B3LYP/6-31+G (d, p) level of theory. The Eigen value of HOMO and LUMO having energy gap ≈ -0.148 eV along with its molecular electrostatic potential (MESP) surface has been evaluated at the same level of theory. The strongest IR vibration, Raman activity, peak in UV-visible absorption band have been calculated to be occurred at 1698 cm⁻¹, 3094 cm⁻¹, 282 nm respectively and (¹H, ¹³C) NMR chemical shifts calculated at the aforesaid theoretical level; are consistent with their experimental counterparts which exhibit the compatibility of the adapted theoretical approach to study this molecular system. The theoretical dipole moment and zero-point vibrational energy has been calculated to be 5.87 Debye & 247.12 Kcal/Mol respectively. The bioactivity of the title molecule has been screened through molecular docking approach and viewed at MESP surface which has been found to be correlated with the molecular orbital theory in terms of low HOMO-LUMO energy gap. The findings of the present investigation enable us to draw the inference that the title bio molecule is a multifunction natural drug agent against the diabetic mellitus and lung cancer.

Keywords— DFT; HOMO-LUMO; IR-Raman; UV-VIS; MESP; Bioactivity

I. INTRODUCTION

Various plant products are being used to treat a variety of disease from the ancient time medicine system such as Ayurveda. This world is enriched with a large number of medicinal plants and modern period may be the right time to use the bio molecules derived from these plants as natural resource using modern science and technology for developing alternative medicines to control the diseases like diabetes, cancer, osteoporosis etc because they will need no cost and labour to synthesize. Iso-Vallesiachotamine is also a naturally occurring compound isolated from the fruits of *Anthocephalus chinensis* plant having molecular formula C₂₁H₂₂N₂O₃ possessing activity against the lung Cancer Cell Line H1299 [1-2], however the physical principle of its bioactivity is yet to be reported. The computational study on the bio molecules has already been emerged as theoretical method to predict its qualitative structure property relationship and same is also required for this molecule because no such study has ever been reported to the best of our knowledge. The computational study on spectroscopic characteristics like IR active vibrations & Raman activity, electronic transitions in UV-Vis spectra, ¹H & ¹³C NMR chemical shifts, thermo chemistry, nonlinear optical

properties and chemical reactivity descriptors has been carried out using density functional theory (DFT) with B3LYP functional and 6-31+G (d, p) basis set. The calculated spectroscopic characteristics have also been compared with their experimental counterparts available in reference 1 and 2 to validate the computationally optimized structure of the title compound. Thermo chemical and nonlinear optical analysis has been performed to predict the related characteristics. Chemical reactivity analysis has been carried out to investigate the physical principle applicable to elucidate its bioactivity.

The present paper contains six sections namely I, II, III, IV, V and VI which discusses introduction, related work, computational methods, results, discussions and conclusion & future scope respectively.

II. RELATED WORK

Density functional theory approach has been adapted to perform the quantum chemistry calculations related to the aforesaid characteristics because of its popularity regarding consistency with the experimental findings in the recent

reports on the bio molecules [3-7]. The drug activity of this bioactive natural molecule has been theoretically explored by using molecular docking which has been reported to be an important theoretical approach for the evaluation of the biological activity [8]. Since, the G Protein (1GCN) receptor and (1X2J & 5C5S) protein receptor have been reported to be a target for an anti diabetic agent [9] and anti lung cancer agent [10] respectively along with G Protein-Coupled receptors are the novel structures for anti diabetic drug [11] hence the binding of the titled molecule as drug agent with these protein receptors has been examined via the same molecular docking reported to be useful in computer-aided drug design due to the importance of shape-matching in drug-macromolecule interactions, as well as the properties of contact surface between the drug and the protein [12]. Docking of this molecule with the human insulin protein receptor (3I40) [13] and pancreatic cancer receptor (2NMO) [14] has also been performed to ascertain its anti diabetic mellitus activity. From the findings of the present investigation, it is inferred that apart from its activity against the lung Cancer Cell Line H1299; it possesses the biological activity against the several types of lung cancer and diabetic mellitus. The findings of the present study may be useful for evolving the principle of the natural bioactivity of the title molecule and developing it as multifunctional drug agent against the diabetic mellitus and lung-cancer.

III. COMPUTATIONAL METHODS

Density Functional Theory Approach

The geometry optimization and frequency calculation were performed at DFT-B3LYP/6-31+G (d, p) level of theory as per reported method [15-16] to carry out the thermo chemical and nonlinear optical analyses. The evaluation of IR and Raman activity were carried out using normal mode analysis of the calculated frequencies at the same theoretical level. The UV-visible absorption spectrum and electronic transitions involved in it were analyzed using the known Time dependent-DFT (TD-DFT) method at the same

theoretical level in ethanol solvent. The ^1H and ^{13}C NMR chemical shifts were calculated by using the well known Gauge Independent Atomic Orbital (GIAO) approach at same level of theory in Dimethyl Sulfoxide (DMSO) solvent. The effect of solvent in TD-DFT and NMR chemical shift were accounted by the reported polarizable continuum model of Tomasi and coworkers [17]. Theoretical calculations of highest occupied molecular orbital (HOMO), lowest unoccupied molecular orbital (LUMO) and molecular electrostatic potential (MESP) surface have been performed using same DFT approach. Gaussian 09 program package [18] has been utilized for implementing the aforesaid theoretical methods.

Molecular docking

The 3D optimized structure of the title molecule obtained by the aforesaid DFT method has been exploited for virtual screening of its bioactivity through molecular docking approach as per the available method using Auto dock 4.2 program packages [19, 20]. The final free energy of binding of this molecule to the receptor has been evaluated as the measure of its drug activity. The free energy of binding is an important parameter in protein-ligand interaction study [21] for predicting the bio molecule to be drug agent. The obtained optimized geometry of the titled compound has been taken as the input ligand to interact with the target protein receptors retrieved from Protein Data Bank (PDB) [22] in the Docking process; results in an interaction energy value and picturizes the interaction energy surface [23].

IV. RESULTS

FT-IR and FT-Raman Analysis

The optimized geometry of the titled molecule consisting of 48 atoms containing nonlinearity due to asymmetric atomic charge distribution has been displayed in Figure 1.

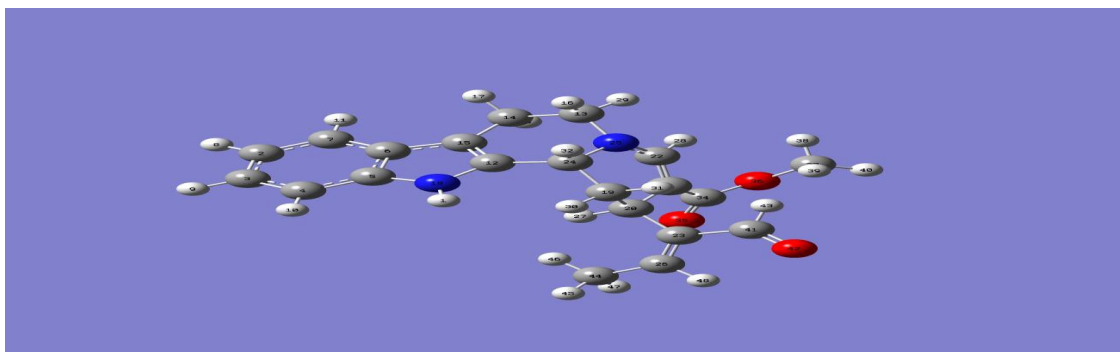


Figure 1 Optimized Geometry of Iso-Vallesiachotamine calculated at B3LYP/6-31+G(d,p)

The normal mode analysis of the vibrational frequency exhibits 138 active fundamental modes of vibration agreeing with the reported formula of maximum $(3N-6)$ numbers of such modes of vibrations in a nonlinear molecule containing N atoms [24]. There is no imaginary frequency in these active modes indicating the existence of true minimum at potential surface. The calculated vibrational frequencies corresponding to these fundamental modes are assigned via gauss-view program [25]. The calculated frequency of each fundamental mode has been scaled with a factor of 0.9648 because the hybrid functional B3LYP in DFT approach tends to overestimate the fundamental modes as reported by Merrick *et al* [26]. The calculated and scaled frequencies of IR active mode of vibrations and its Raman activity have been depicted in Table 1. The theoretical IR and Raman Spectra have been displayed in Figure 2 and Figure 3 respectively.

NMR analysis

The comparison of theoretical and experimental values of ^{13}C NMR and ^1H NMR chemical shifts provides a schematic approach for the structural prediction of large bio molecules [27]. The difference between isotropic magnetic shielding (IMS) of tetramethylsilane (TMS) and any proton (x) given by $\delta x = \text{IMS}_{\text{TMS}} - \text{IMS}_x$ predicts the chemical shift of that proton. The calculated values of ^1H and ^{13}C chemical shifts have been depicted in Table 2 and are in good agreement with the reported experimental values. The ^1H chemical shift for 28H largely differed with the experimental values, may be because of other shielding effects arising due to the space orientation at the optimized geometry.

The chemical structure including the computationally assigned serial number of the atoms in the optimized geometry of the title molecule used for NMR chemical shift calculation has been displayed in Figure 4.

UV-Visible absorption analysis

The UV-Visible spectra obtained using TD-DFT method in ethanol solvent has been shown in Figure 5. We have analyzed the excited states by specifying the excitation energies, wavelengths and oscillator strengths listed in Table 3. The oscillator strength is the measurement of how strongly the particular electronic transition is allowed in absorption. The maximum absorption intensity occurs at 282.03 nm at excitation energy 4.3961 eV corresponding to the orbital transitions $\text{H}-1 \rightarrow \text{L}+1$, $\text{HOMO} \rightarrow \text{L}+2$ with oscillator strength 0.211. This oscillator strength is largest amongst all and hence these transitions would be the strongly allowed.

Thermo chemical analysis

By default, the program package used in the present study carries out thermo chemical analysis at 298.15 K temperature and 1 atmosphere of pressure wherein the parameters namely

thermal energy correction (E), molar heat capacity at constant volume (C_V) and entropy (S) for electronic, translational, rotational and vibrational components have been depicted in table 4. The electronic component of these parameters is zero due to the lack of free electrons in this molecule. The translational and rotational thermal energy correction is negligibly small and thermal correction to the energy is practically accounted by the vibrational component. The molecular mass of the title compound has been estimated to be 350.16304 amu and its zero-point vibrational energy is 247.12374 Kcal/Mol. The total energy of this molecular system is represented by $E_{\text{total}} = E_0 + E_{\text{vibrational}} + E_{\text{rotational}} + E_{\text{translational}}$, where $E_0 = E_{\text{electronic}} + \text{zero-point energy}$. Zero-point energy correction to the electronic energy accounts for the effect of vibrations persisting even at 0 K in the molecule which has been estimated to be 247.12 Kcal/Mol. The final electronic energy has been predicted to be $E_0 = -720570.04$ Kcal/Mol. Since, the thermal correction to Energy = 261.90 Kcal/Mol, to Enthalpy = 262.49 Kcal/Mol and to Gibbs free energy = 213.14 Kcal/Mol has been predicted and hence the final electronic energy E_0 , Enthalpy $H = E + RT$ and Gibbs free energy $G = H - TS$ are subject to the thermal correction.

Finally, the sum of electronic and thermal Energies = -720555.26 Kcal/Mol, sum of electronic and thermal Enthalpies = -720554.67 Kcal/Mol and sum of electronic and thermal Free Energies = -720604.02 Kcal/Mol has been predicted by the said theoretical computation.

Nonlinear optical analysis

The total energy has been calculated at the single point of the molecular potential surface at optimized geometry named as the single point energy which is -1148.68 Hartree at equilibrium. Total calculated dipole moment is 5.87 Debye distributed along x, y and z as -4.1201, -2.3912 and -3.4326D respectively, mean polarizability (α) = 0.293×10^{-23} esu and the mean first order hyperpolarizability (β) = 11.495×10^{-30} esu indicating the axial and trans-axial distortion exist in the title molecule which may produce nonlinear effects.

Chemical reactivity analysis

The calculated values of chemical reactivity descriptors are: ionization potential = 0.21626 eV, electron affinity = 0.06759 eV, chemical hardness = 0.074 eV, chemical potential = -0.141 eV, electro negativity = 0.141 eV and electrophilicity index = 0.134 eV. Pearson proposed the HOMO-LUMO energy gap to be the measure of softness of molecule for chemical reaction [28] which has been calculated to be -0.1486 eV, reasonably small in title molecule. The ability of electron transportation and excitation properties is qualitatively predicted through HOMO and LUMO [29] wherein HOMO primarily acts as an electron donor and LUMO acts as an electron acceptor and tends to create chemical reactivity through electronic transition [30]. The

HOMO and LUMO plots of the title compound have been shown in Figure 6.

MESP surface is very useful to understand the potential sites for electrophilic (negative region) and nucleophilic (positive region) reactions [31] which is well suited for recognition of one molecule by another through this potential, as in the case of drug-receptor interactions [32] shown in Figure 7. The values of the electrostatic potential at the surface are displayed by different colors in the order of red < orange < yellow < green < blue. The color code of these maps is in the range between -8.503 a.u. (deepest red) and 8.503 a.u. (deepest blue) in the titled compound, where blue indicates the most electropositive i.e. electron poor region and red indicates the most electronegative region, i.e. electron rich region. From the MESP figure it is evident that the most electronegative region is located around oxygen atom attached to carbon atom which effectively acts as electron donor in molecule.

Bioactivity analysis

The binding of Vallesiachotamine molecules as a ligand with 1GCN, 2NMO, 3I40, 1X2J and 5C5S protein receptors has been observed to be mediated through the O-atoms of the titled ligand molecule at all the residues sites. Intermolecular and the free energy of binding of this ligand (titled molecule)-protein (receptors) interaction calculated by molecular docking approach depicted in Table 5 have been observed to be significantly negative in case of the entire ligand-protein complex. The biological activity of this molecule evaluated in this study explores its drug application.

V. DISCUSSION

The normal mode analysis of IR active vibrations is specific feature of theoretical computation and not possible through experimental methods. The vibrations in the region 3093.95-3006.33 cm^{-1} occurring at the active modes of vibrations 137-129 as obvious from the table 1, are observed to be C-H stretching which in agreement with earlier reported characteristic region (3100-3000 cm^{-1}) [33] appeared due to the aromatic ring. The vibrational modes 89-65 shows the frequency range 1303.70-1020.06 cm^{-1} which correspond to C-H in plane bending frequencies appearing in line with the reported range 1300-1000 cm^{-1} [34]. The C-H out of plane bending vibrations have been reported to be appearing in the region 1000-750 cm^{-1} [35] which are aligned with the theoretical vibrations occurred at the active modes 64-48 in the region 1004.63-751.27 cm^{-1} . Thus, the theoretically evaluated regions for C-H vibrations are in good agreement with their experimental counterpart. The C-C stretching vibrations in titled compound are found in the region 1604.74-1426.55 cm^{-1} corresponding to the vibrational mode 112-99. The low region frequencies of other vibrational modes which are hardly observed in experiments have also

been calculated through the said theoretical approach. The theoretical IR spectra exhibit the maximum intensity at 1699 cm^{-1} which is in good agreement with the earlier experimental findings. The strongest Raman activity has been observed at 3094 cm^{-1} which is the characteristics of this molecule. The calculated ^1H and ^{13}C chemical shifts in NMR analysis are in good agreement with the experimental values. The UV-Visible analysis predicts four electronic transitions involved in producing UV-visible absorption band out of which the maximum peak occurs at 282 nm leading to an excellent agreement with its experimental value 291 nm. The prediction of the electronic transitions, oscillator strengths and excitation energies corresponding to the absorption band in UV spectrum, is an important advantage of the present study.

Thermo chemical analysis predicts the statistical mechanical descriptors to be used for describing the phase transition in the chemical reaction of the title molecule which in turns indicate the causes of its natural biological activity. The chemical reactivity descriptors predict the title molecule to be a soft molecule for chemical reaction in terms of a reasonably small energy gap between HOMO-LUMO energy level causing its bioactivity as per the earlier study of Pearson quoted in reference no. 27. In this way the phenomenon of its natural bioactivity is correlated with the molecular orbital theory. Since MESP surface has electron rich region located around O-atom is a good reactive site; agree with the report quoted in references 4 and 5 and hence the binding of Vallesiachotamine molecules as a ligand with protein receptors has been observed to be mediated through the O-atoms of the titled molecule at all the residues sites which again confirms that its natural bioactivity is correlated with the molecular orbital theory.

VI. CONCLUSION & FUTURE SCOPE

The calculated vibrational spectroscopic characteristics at B3LYP/6-31+G (d,p) level are aligned well to other reported results as obvious by the discussion section of this paper and the strongest IR active & Raman activity occur at the wave numbers 1698 & 3094 cm^{-1} respectively. The calculated values of the NMR chemical shift in the title molecule at the same theoretical level are also in good agreement with their experimental counterparts. The electronic spectra of UV-Visible spectrum predict the various possible intra molecular charge transfer out of which the molecular transition HOMO-1 \rightarrow L+1, HOMO \rightarrow L+2 corresponds to the maximum peak at 282 nm which is in good agreement with its experimental value 291 nm. The thermo chemical analysis predicts the zero-point vibrational energy in Iso-vallesiactomine to be 247.12 Kcal/Mol. The dipole moment has been calculated to be 5.8716 Debye which indicates the axial and trans-axial distortion in the shape of the title molecule to produce nonlinear effects. HOMO-LUMO energy gap in this molecule is significantly low (\approx -0.1486 eV) which makes it best fit for being chemically reactivity. The bioactivity of the

title molecule is thus correlated with the molecular orbital theory in terms of HOMO-LUMO energy gap as per the findings of reference 28. A free binding energy value -5.26 kcal/mol, -5.94 kcal/mol, -6.37 kcal/mol, -7.43 kcal/mol and -5.90 kcal/mol have been predicted with the help of molecular docking with 1GCN, 1X2J, 2NMO, 3I40 and 5C5S receptors respectively which reveals that the titled molecule possesses multifunctional anti diabetic and anti-lung cancer drug activity. The binding of this molecule in entire ligand-protein complex screened for its bioactivity analysis has been observed to be mediated through O-atom; this is because

electron rich region is located around O- atom as obvious from the MESP surface containing reasonably low HOMO-LUMO energy gap which again confirms that the physical principle of its bioactivity is correlated with the molecular orbital theory. Hence it is concluded that the molecular orbital theory forms the basis of the physical principles of the phenomenon of the natural bioactivity of the title molecule. We propose the molecular dynamics simulation study to be the future scope of the present study for exploring its drug related applications .

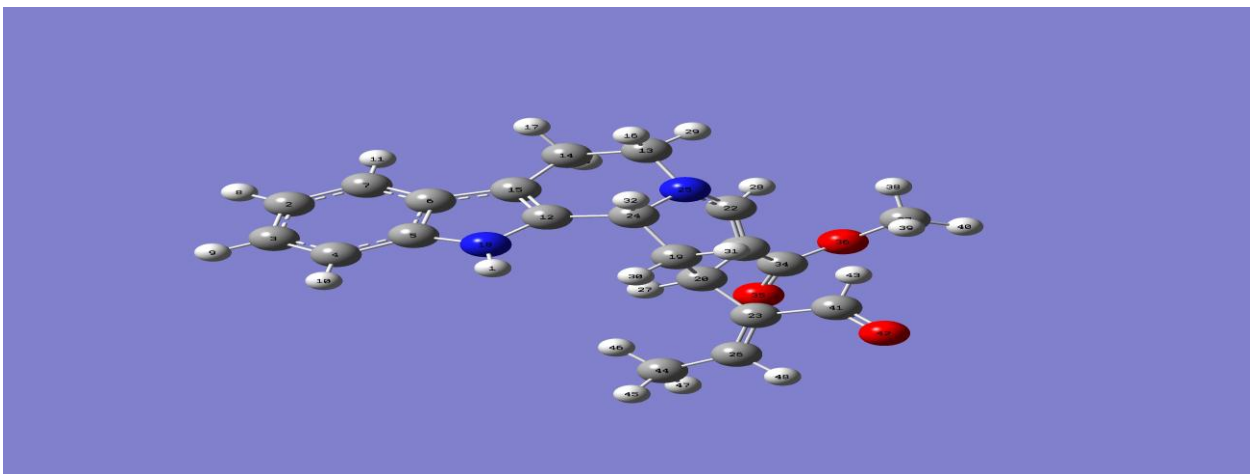


Figure 1 Optimized Geometry of Iso-Vallesiachotamine calculated at B3LYP/6-31+G(d,p) level

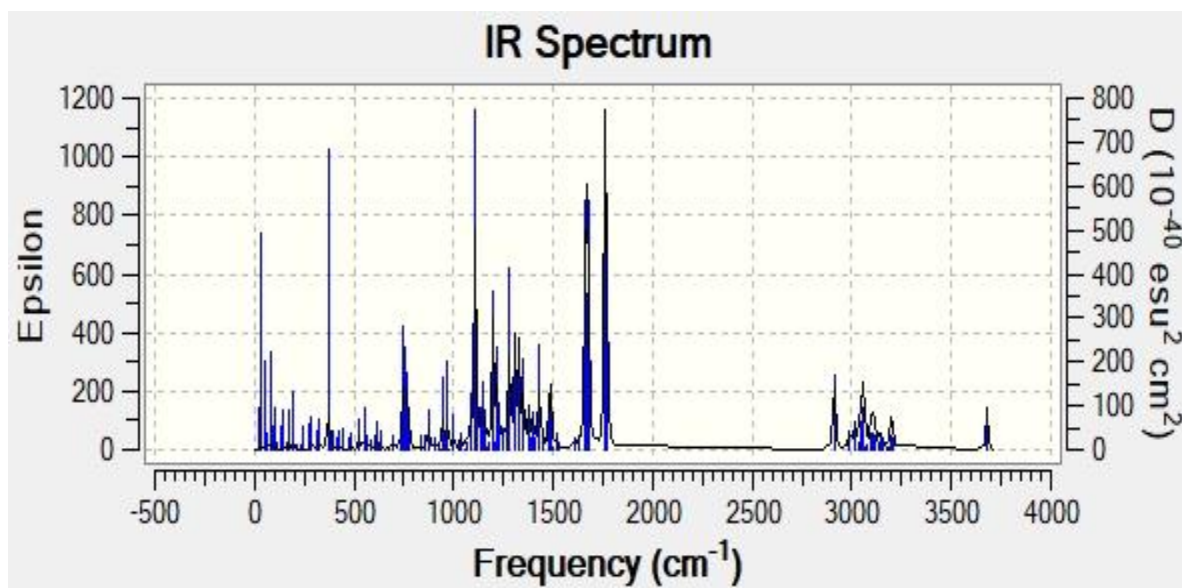


Figure 2 IR spectra of Iso-Vallesiachotamine obtained at B3LYP/6-31+G (d, p) level.

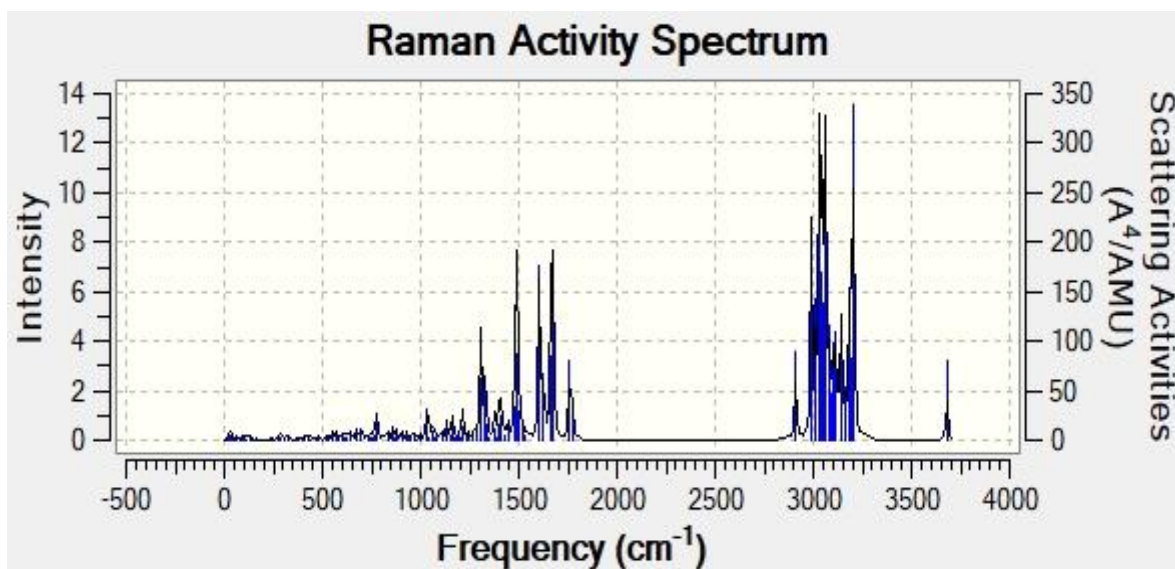


Figure 3 Raman spectra of Iso-Vallesiachotamine obtained at B3LYP/6-31+G (d, p) level.

Table 1 IR active vibrations and Raman activity in Vallesiachotamine obtained by normal mode analysis at B3LYP/6-31+G(d,p) level

Active mode of vibrations	Calculate d freq.(cm ⁻¹)	Scaled freq.(cm ⁻¹)	Intensity IR	Vibration Description	Raman Activity (A ⁴ /AMU)	D-Dipolar	U-Dipolar
1	22.00	21.23	0.5283	τ_i (H38-H39)	2.2266	0.6943	0.8196
2	27.88	26.90	0.4432	τ_o (H46-H47-H48-C44)	3.5561	0.6624	0.7969
3	35.90	34.64	4.4479	τ_o (C44-H45-H47) + τ_i (O42)	3.9496	0.7111	0.8312
4	54.28	52.37	2.7428	τ_i (C37-H38-H39-H40)	1.2086	0.6562	0.7924
5	66.05	63.73	0.6153	R[τ_o (H33-H11) + τ_i (H10-H1)]	4.7487	0.7458	0.8544
6	80.38	77.55	4.5271	τ_o (H45-H47)+ τ_i (O35-H39)	1.8382	0.7209	0.8378
7	94.79	91.45	1.2275	τ_o (H46-H47)+ τ_i (H38)	2.8820	0.7387	0.8497
8	98.77	95.29	2.3274	τ_o (H39-H8) + τ_i (O36)	1.8294	0.6912	0.8174
9	116.47	112.37	0.5408	τ_o (H39-H38-H40)	0.4253	0.6717	0.8036
10	128.31	123.79	0.2505	τ_o (H45-H47)+ τ_i (H46)	0.7299	0.1154	0.2069
11	133.04	128.36	1.8539	τ_o (H45-H47)+ τ_i (H46)	1.1455	0.6314	0.7741
12	138.32	133.45	3.1797	τ_o (H39-H43)	0.9223	0.6226	0.7674
13	161.24	155.56	0.6173	R[τ_o (H30-H31)+ τ_i (H43)]	1.3464	0.7148	0.8337
14	174.81	168.66	3.9593	R[τ_o (H33-H17)]	0.8583	0.5209	0.6850
15	192.49	185.71	6.4998	τ_o (H45-H46)+ τ_i (H43)	1.0771	0.5980	0.7485
16	209.25	201.88	0.6883	τ_o (C44-H45-H46)]	0.7113	0.7470	0.8552
17	232.39	224.21	0.5830	R[τ_o (H16-H29-H33)]	1.3441	0.1962	0.3280
18	247.05	238.35	3.3127	τ_o (H47-H43)] + τ_i (C26-H48)	1.5653	0.7457	0.8543
19	275.10	265.42	4.0347	R[τ_o (H30-H31)+ τ_i (H1)]	1.3405	0.1917	0.3217
20	281.37	271.47	0.5025	R[τ_o (N18) + τ_i (H33-H17)]	0.7017	0.0951	0.1738
21	285.12	275.08	5.1559	R[τ_o (H1) + τ_i (H17-H33)]	2.4329	0.6551	0.7916

22	310.68	299.74	3.2999	$R[\tau_o (H16-H28-H29)]$	1.8990	0.2037	0.3385
23	323.89	312.49	5.5357	$R[\tau_o (H1) + \tau_i (H30-H31)]$	2.7235	0.1143	0.2051
24	369.64	356.63	63.1510	$R[\tau_o (H1) + \tau_i (H16)]$	0.8535	0.7279	0.8425
25	379.15	365.80	3.4266	$R[\tau_o (H1-H17-H33) + \tau_i (H16-H29)]$	1.6333	0.5345	0.6967
26	393.44	379.59	4.1691	$R[\tau_o (H1-H30)] + \tau_i (H29-H39)$	2.1594	0.2797	0.4371
27	410.14	395.70	2.6210	$R[\tau_o (H30-H31)]$	2.9030	0.7406	0.8509
28	426.20	411.20	4.7370	$R[\tau_o (H16-H28) + \tau_i (H29)]$	2.2182	0.3459	0.5140
29	439.21	423.75	5.1367	$R[\tau_o (H10-H11)]$	0.3769	0.4711	0.6404
30	476.56	459.79	3.1814	$R[\tau_i (H31)] + \tau_o (H45-H46) + \tau_i (C26)$	0.9792	0.7081	0.8291
31	483.97	466.93	4.6652	$R[\tau_i (H31-H33-H17)]$	2.5575	0.7386	0.8496
32	523.81	505.37	93424	$R[\tau_i (H17-H33)] + \tau_o (H43-H48) + \tau_i (C23)$	2.6241	0.2723	0.4281
33	528.81	510.20	9.1804	$R[\tau_o (H1-H33-H17) + \tau_i (H10-H32)]$	1.8137	0.6023	0.7518
34	549.96	530.60	13.1697	$R[\tau_o (H27-H32) + \tau_i (H30-C19)]$	4.7861	0.1632	0.2805
35	568.3	548.30	4.7088	$R[\tau_o (H1-H32) + \tau_i (H31)]$	7.007	0.1558	0.3134
36	583.44	562.90	3.0759	$R[\tau_o (H1-H9) \tau_i (H8)]$	0.1666	0.7194	0.8368
37	606.01	584.68	4.7528	$R[u_s (C2-C4) + \tau_i (H8-H9)]$	6.0820	0.7500	0.8571
38	611.72	590.19	9.5006	$R[\tau_o (H17-H33)]$	1.3544	0.4637	0.6336
39	623.66	601.71	2.868	$R[\tau_o (H27-H28) \tau_i (H29)]$	2.0141	0.6853	0.8132
40	638.06	615.60	6.9825	$R[\tau_o (H33-H16)] + \tau_i (O35-C34-H38)]$	9.2882	0.0351	0.0678
41	676.72	652.90	1.1795	$u_s (C12-C15) + \tau_o (H1-H10-H8)$	10.4890	0.0282	0.0548
42	698.66	674.07	5.3336	$R[\tau_o (C20-H27)] + \tau_i (H30-H31)]$	11.6250	0.2489	0.3986
43	730.88	705.15	4.6907	$R[\tau_o (H1-H33) + \tau_i (H16-H29)]$	4.7788	0.7481	0.8559
44	745.49	719.25	52.0738	$R[\tau_o (H8-H10-H16)]$	1.6787	0.3595	0.5289
45	755.20	728.62	44.1201	$R[\tau_i (H8-H9-H10-H11)]$	2.2811	0.6931	0.8188
46	765.88	738.92	33.7426	$R[\tau_o (H11) + \tau_i (H10)] + \tau_o (C34)$	4.1081	0.1951	0.3265
47	770.00	742.90	30.9253	$R[\tau_o (H30-H31)] + \tau_i (C6-H10)$	0.4886	0.7330	0.8459
48	778.68	751.27	18.9760	$\tau_o (H45-H47) + \tau_i (C41-H43)$	23.3578	0.0486	0.0926
49	832.10	802.81	7.0458	$\tau_o (H11-H33) + \tau_i (H17)$	8.1982	0.1214	0.2165
50	857.81	827.62	1.0677	$R[\tau_o (H8-H11) + \tau_i (H9-H10)]$	2.0482	0.2720	0.4276
51	860.12	829.84	6.3718	$R[\tau_o (H1-H30) + \tau_i (H27-H31)]$	7.6188	0.0367	0.0709
52	872.37	841.66	19.2519	$\tau_i (H47-H48)$	2.3267	0.3331	0.4998
53	875.54	844.72	9.7116	$\tau_o (H1-H30) + \tau_i (H31-H27)$	5.9140	0.5831	0.7367
54	903.75	871.94	5.9941	$R[\tau_o (H16-H29-H33)]$	9.6128	0.2524	0.4030
55	927.65	895.00	2.2614	$R[\tau_o (H30-H31-) + \tau_i (H17-H32)]$	4.8239	0.4465	0.6174
56	938.28	905.25	0.5466	$R[\tau_o (H8-H9) + \tau_i (H11-H10)]$	0.9981	0.7280	0.8426
57	943.81	910.59	38.6113	$R[\tau_o (H28)]$	1.2574	0.5928	0.7444
58	953.05	919.50	5.1759	$R[u_{as} (C14-C13) + \tau_o (H17-H29-H33)]$	5.2453	0.5769	0.7317
59	970.58	936.42	49.0939	$R[\tau_o (H28-H30)]$	4.1378	0.5713	0.7272

60	978.25	943.82	0.0169	$R[\tau_o (H9-H11) + \tau_i (H8-H10)]$	0.1790	0.7254	0.8408
61	1001.63	966.37	19.6815	$R[\tau_o (H31-H27)] + \tau_o (H45-H48)$	3.0850	0.0166	0.0327
62	1026.32	990.19	2.5355	$R[\tau_o (H32)] + \tau_i (H43)$	5.9256	0.2113	0.3488
63	1035.40	998.95	10.0389	$u_s (C2-C3) + \tau_o (H11-H10-H9-H8)$	30.9116	0.0734	0.1367
64	1041.28	1004.63	2.4542	$R[\tau_o (H32)] + \tau_i (H43)$	2.7489	0.4047	0.5763
65	1057.28	1020.06	0.5684	$R [(H27-H31) + (H30-H32)]$	8.1833	0.2081	0.3444
66	1064.98	1027.49	4.1771	$R[\tau_o (H16-H33) + \tau_i (H17)]$	4.4425	0.2324	0.3771
67	1070.01	1032.35	0.9407	$\tau_o (H48) + \tau_i (H45-H47)$	2.8868	0.6823	0.8111
68	1084.28	1046.11	35.2071	$R[\tau_o (H17-H30) + \tau_i (H31-H32)]$	6.4082	0.4110	0.5825
69	1107.79	1068.80	215.318	$u_{as} (O36-C34) + \tau_o (H39-H30)$	9.3133	0.7385	0.8496
70	1116.07	1076.78	28.6320	$R[u_{as} (C20-C23)] + \tau_o (H46-H43)$	2.3258	0.7068	0.8282
71	1133.83	1093.92	27.0374	$R[\tau_o (H8-H9) + \tau_i (H10-H11)]$	12.4954	0.2050	0.3403
72	1149.96	1109.48	43.7716	$R[u_{as} (N25-C13) + \tau_o (H8-H9) + \tau_i (H10)]$	3.9391	0.6834	0.8120
73	1161.74	1120.85	25.8995	$R[\tau_o (H32-H9) + \tau_i (H10-H30)]$	17.1412	0.2145	0.3532
74	1171.36	1130.13	0.9955	$\tau_o (H38-H40) + \tau_i (H39)$	1.5958	0.4450	0.6159
75	1179.57	1138.05	5.1372	$R[\tau_o (H10-H11) + \tau_i (H8-H9)]$	2.2134	0.4683	0.6379
76	1197.65	1155.49	107.850	$R[\tau_o (H33-H31-H29) + \tau_i (H1-H27)]$	5.7620	0.1361	0.2397
77	1200.79	1158.52	29.4054	$R[\tau_o (H33-H16-H29) + \tau_i (H17)]$	3.2090	0.3927	0.5640
78	1212.44	1169.76	4.8003	$R[\tau_o (H33-H17)] + \tau_i (H39-H40)$	12.3440	0.1865	0.3144
79	1215.16	1172.39	70.5086	$R[\tau_o (H1-H33) + \tau_i (H17-H31)]$	9.9170	0.1138	0.2043
80	1230.39	1187.08	27.9743	$R[\tau_o (H1-H17) + \tau_i (H29)]$	1.4139	0.5310	0.6937
81	1242.87	1199.12	14.9532	$R[\tau_o (H1-H29-H32) + \tau_i (H17)]$	5.0989	0.0854	0.1573
82	1263.19	1218.73	19.4672	$R[\tau_o (H11-H29-H33) + \tau_i (H10)]$	3.9651	0.7382	0.8494
83	1280.85	1235.76	132.308	$R[\tau_o (H32) + \tau_i (H27)]$	13.8305	0.7500	0.8571
84	1305.90	1259.93	37.5770	$R[\tau_o (H32-H27)]$	29.5037	0.6136	0.7605
85	1308.67	1262.60	78.1400	$R[u_{as} (C4-C3) + \tau_o (H32-H9)]$	62.4335	0.2548	0.4061
86	1325.16	1278.51	64.5940	$R[\tau_o (H27-H30-H32)]$	3.8738	0.3887	0.5598
87	1329.80	1282.99	52.8939	$R[\tau_o (H27-H32-H33)]$	50.5575	0.1379	0.2423
88	1332.63	1285.72	33.8370	$R[\tau_o (H29-H30) + \tau_i (H32-H27)]$	16.1661	0.5073	0.6731
89	1351.26	1303.70	70.7473	$R[\tau_o (H30-H32) + \tau_i (H16)]$	2.31116	0.6499	0.7878
90	1375.42	1327.01	15.7014	$R[\tau_o (H29-H16)] + \tau_i (H48)$	5.7769	0.7445	0.8535
91	1377.50	1329.01	27.3619	$R[\tau_o (H16-H29)] + \tau_i (H48)$	12.0485	0.3567	0.5258
92	1384.56	1335.82	9.1852	$R[\tau_o (H27-H28) + \tau_i (H31-H32)]$	2.2014	0.5925	0.7441
93	1395.37	1346.25	9.2795	$R[\tau_o (H29-H31-H32)]$	14.7477	0.1918	0.3218
94	1401.67	1352.33	29.3758	$R[\tau_o (H28-H29)]$	14.2255	0.3741	0.5445
95	1405.31	1355.84	2.3586	$R[\tau_o (H9-H32-H31)]$	16.8695	0.4149	0.5864
96	1412.72	1362.99	9.9369	$\tau_o (H45-H46-H47)$	24.4594	0.3340	0.5007
97	1431.55	1381.16	85.5851	$R[\tau_o (H32-H16) + \tau_i (H29)]$	3.9564	0.4061	0.5777

98	1445.44	1394.56	15.5618	τ_o (H43-H48)	17.1238	0.5980	0.7484
99	1478.60	1426.55	0.6360	τ_o (H47)+ τ_i (H45-H46)	6.8780	0.4644	0.6343
100	1479.96	1427.87	16.5681	$R[u_s(N18-C12)]+\tau_i$ (H9-H10)] τ_o (H47)	10.9240	0.7075	0.8287
101	1481.26	1429.12	22.9118	τ_o (H39-H40)	8.8853	0.7245	0.8402
102	1484.67	1432.41	14.1676	τ_o (H47)+ τ_i (H45-H46)	32.3804	0.3035	0.4656
103	1488.74	1436.34	41.7626	$R[u_s(N18-C5-C6)]+\tau_i$ (H10-H11)]	88.0078	0.5769	0.7317
104	1489.81	1437.37	3.5724	τ_o (H16)+ τ_i (H17-H33)	17.1827	0.4172	0.5888
105	1492.99	1440.44	1.6653	τ_o (H38-H39-H40)	4.4108	0.6956	0.8505
106	1493.39	1440.82	4.0036	$R[\tau_i$ (H30-H31)]	20.8363	0.6110	0.7585
107	1501.77	1448.91	1.7907	$R[\tau_o$ (H29-H16)]	29.3629	0.5766	0.7314
108	1515.99	1462.63	14.7265	τ_o (H38-H40)	16.5990	0.4950	0.6622
109	1527.25	1473.49	3.6025	$R[u_{as}(C2-C7) + \tau_o$ (H8-H9-H1)]	4.5167	0.6530	0.7900
110	1605.04	1548.54	98845	$R[u_{as}(C4-C5)+u_s\{(C15-C12)+(C2-C3)\}]$	176.127	0.3699	0.5400
111	1627.16	1569.88	9.0099	$R[u_{as}(C12-C15)+u_s\{(C5-C6)+(C2-C3)\}]$	66.6009	0.1835	0.3102
112	1663.29	1604.74	235.412	$R[u_s(C21-C22)+ (C4-C5)+(C2-C7)]$	83.7078	0.2092	0.3460
113	1667.68	1608.98	148.482	$R[u_{as}(C4-C5)+u_s\{(C12-C15)+(C2-C7)\}]$	48.9220	0.6000	0.7500
114	1675.53	1616.55	238.333	$R[u_s(C21-C22)]+ u_s(C23-C26)+(C41-O42)$	140.250	0.0546	0.1035
115	1759.66	1697.72	320.463	$u_s(C34-O35)$	80.9175	0.3068	0.4696
116	1771.78	1709.41	153.606	$u_s(C41-C42)+ u_s(C23-C26)$	40.4638	0.6617	0.7964
117	2911.20	2808.73	124.609	$u_s(C41-H43)$	89.6496	0.2804	0.4379
118	2990.09	2884.84	31.257	$R[u_s(C24-H32)]$	216.878	0.1686	0.2886
119	3013.34	2907.27	32.1590	$R[u_s(H17-C14-H33)]$	142.308	0.0943	0.1723
120	3031.26	2924.56	14.0658	$u_s(H48-C45-H47)$	297.602	0.1043	0.1888
121	3041.58	2934.52	47.4307	$R[u_s(H38-C37-H40-H39)]$	168.660	0.0616	0.1161
122	3047.92	2940.63	8.4050	$R[u_s\{(H17-C14)+(H29-C13)\}]$	76.0410	0.5919	0.7436
123	3055.12	2947.58	27.8229	$R[u_s(H30-C19-H31)]$	137.625	0.0634	0.1193
124	3060.36	2952.64	74.4990	$R[u_s\{(H17-C14)+(H29-C13)\}]$	258.052	0.1479	0.2577
125	3066.27	2958.34	3.8779	$R[u_s(H27-C20)]$	44.7861	0.2590	0.4114
126	3078.63	2970.26	7.9223	$u_s(H45-C44-H47)$	115.720	0.7350	0.8473
127	3094.67	2985.74	29.8538	$R[u_s(H30-C19-H31)]$	47.623	0.7425	0.8522
128	3106.09	2996.76	27.6888	$R[u_s(H16-C13-H29)]$	98.2025	0.6604	0.7955
129	3116.01	3006.33	26.1684	$u_s(H38-C37)+ u_{as}(H38-C37-H40)$	109.495	0.5052	0.6712
130	3139.56	3029.05	12.5363	$u_s\{(H46-C44)+ (C26-H48)\}]$	95.7852	0.4674	0.6371
131	3141.84	3031.25	20.5522	$u_s\{(H39-C37-H40)\}]$	67.2307	0.5937	0.7450
132	3159.99	3048.76	11.1050	$u_s\{(H46-C44)+ (C26-H48)\}]$	53.9163	0.1821	0.3081
133	3178.87	3066.97	2.2393	$R[u_s\{(H10-C4)+H9-C3)+(H8-C2)+(H11-C7)\}]$	21.6468	0.6656	0.7992
134	3184.35	3072.26	2.2297	$R[u_s\{(H10-C4)+(H11-C7)\}]$	127.356	0.6572	0.7931

135	3195.14	3082.67	25.6190	R[$\nu_s\{(H10-C4)+H9-C3)+(H11-C7)\}$]	82.1318	0.7477	0.8556
136	3197.46	3084.91	5.8841	R[$\nu_s(C22-H28)$]	60.3647	0.3335	0.5002
137	3206.83	3093.95	22.3885	R[$\nu_s\{(H10-C4)+H9-C3)+(H8-C2)+(H11-C7)\}$]	339.910	0.144	0.2517
138	3680.46	3550.91	50.9529	R[$\nu_s(N18-H1)$]	79.494	0.1469	0.2562

Abbreviations:- ν_{as} : asymmetric stretching, ν_s : symmetric stretching, τ_o : out of plane torsion, τ_i : in the plane torsion, R: carbon ring.

Note: The vibrations whose potential energy distributions are less than 20% have been neglected for the sake of simplicity.

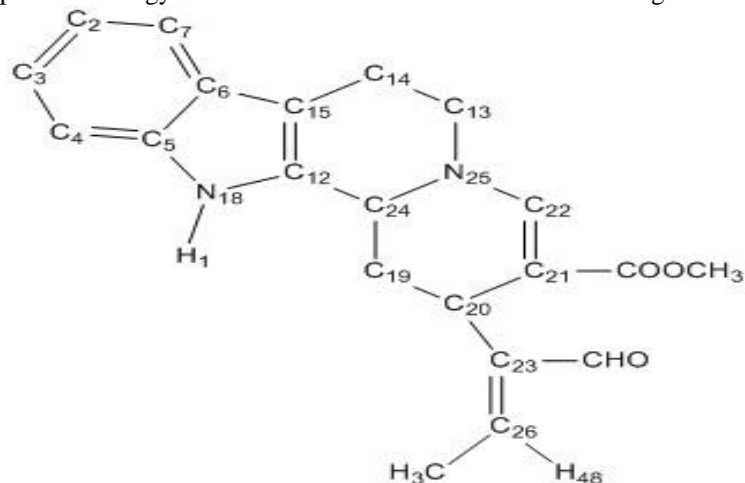


Figure 4 Chemical structure view of the optimized structure of Iso-Vallesiachotamine in NMR analysis

Table 2 Comparison of theoretical and experimental (1H NMR, ^{13}C) chemical shift (δ ppm) in Vallesiachotamine

Position of Atom	Δ cal (ppm)	δ exp* (ppm)	Degeneracy & assignments	Position of Atom	δ cal (ppm)	δ exp* (ppm)	Degeneracy & assignments
2C	112.44	120.1	1(Aromatic Ring)	24C	50.43	49.2	1(Out of Ring)
3C	108.43	122.5	1(Aromatic Ring)	26C	141.39	147.8	1(Methene Group)
4C	102.68	112.2	1(Aromatic Ring)	27H	3.32	4.29	1
5C	135.31	138.8	1(Pyrrole Ring)	28H	19.09	7.33	1
6C	114.57	127.8	1(Pyrrole Ring)	29H	3.59	3.74	1
7C	104.88	118.8	1(Aromatic Ring)	30H	1.84	1.26	1
8H	7.61	6.99	1	31H	2.50	1.26	1
9H	7.56	7.06	1	32H	4.58	4.29	1
10H	7.70	7.28	1	33H	2.74	NA	1
11H	7.82	7.40	1	34C	166.58	170.3	1(Acid Group)
12C	147.79	138.1	1	37C	60.64	51.3	1(Acid Group)
13C	40.69	52.2	1(Aromatic Ring)	38H	14.12	NA	1(Acid Group)
14C	21.09	23.0	1(Aromatic Ring)	39H	3.64	3.61	1(Acid Group)
15C	111.62	108.3	1(Pyrrole Ring)	40H	3.42	NA	1(Acid Group)
16H	3.21	3.74	1	41C	187.51	192.0	1(-CHO Group)
17H	2.31	2.81	1	43H	10.29	10.26	1(-CHO Group)
19C	17.04	30.6	1(Aromatic Ring)	44C	NA	13.3	1(-C ₂ H ₄ Group)
20C	25.44	49.1	1(Aromatic Ring)	45H	1.09	2.18	1(-C ₂ H ₄ Group)
21C	96.01	94.5	1(Aromatic Ring)	46H	1.47	2.18	1(-C ₂ H ₄ Group)
22C	139.49	149.6	1(Aromatic Ring)	47H	1.52	2.18	1(-C ₂ H ₄ Group)
23C	134.71	144.5	1(Aromatic Ring)	48H	8.29	6.55	1(-C ₂ H ₄ Group)

*Source: Reference [1, 2]

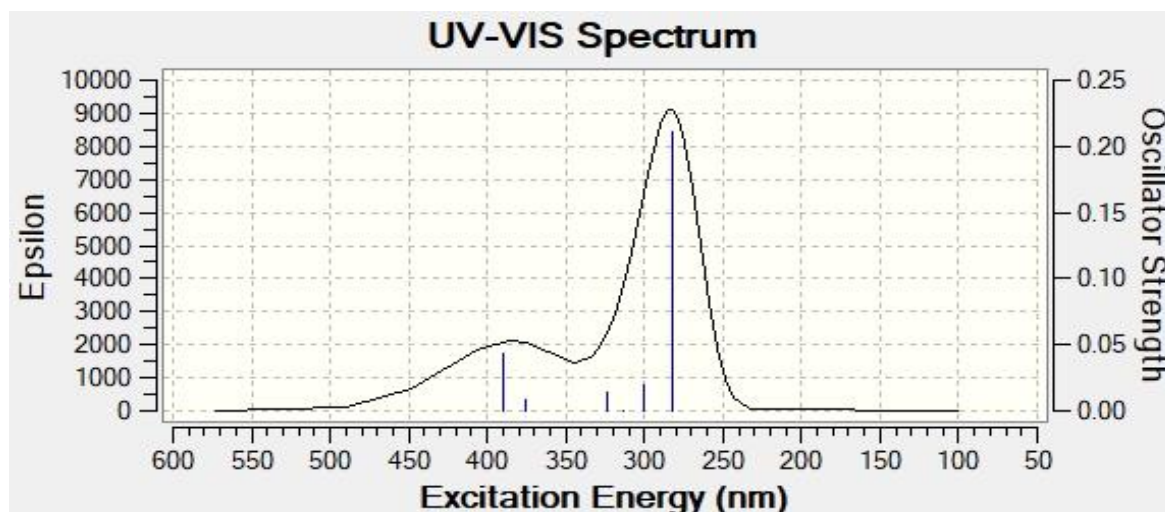


Figure 5 UV-Visible spectra of Iso-Vallesiachotamine obtained at B3LYP/6-31+G (d, p) level

Table 3. TDDFT analysis of UV-visible spectrum of Iso-Vallesiachotamine obtained at B3LYP/6-31+G(d,p) level.

S No.	Excitation Energy(eV)	Wavelength(nm)	Oscillator Strength	Orbital transition
1	3.8349	323.3	0.0134	H-4→LUMO
2	3.9514	313.77	0.0003	H-2→LUMO
3	4.1201	300.92	0.0189	HOMO→L+1
4	4.3961	282.03	0.211	H-1→L+1,HOMO→L+2

Table 4: Thermo chemical parameters of Iso-Vallesiachotamine obtained at B3LYP/6-31+G (d, p) level

S.No	Components	E (Thermal) KCal/Mol	C _v Cal/Mol- Kelvin	S Cal/Mol- Kelvin
1	Electronic	0.000	0.000	0.000
2	Translational	0.889	2.981	43.454
3	Rotational	0.889	2.981	35.394
4	Vibrational	260.129	84.531	86.677
5	Total	261.906	90.493	165.525

HOMO (-0.21626 eV)

LUMO (-0.06759 eV) (Energy difference = - 0.1486 eV)

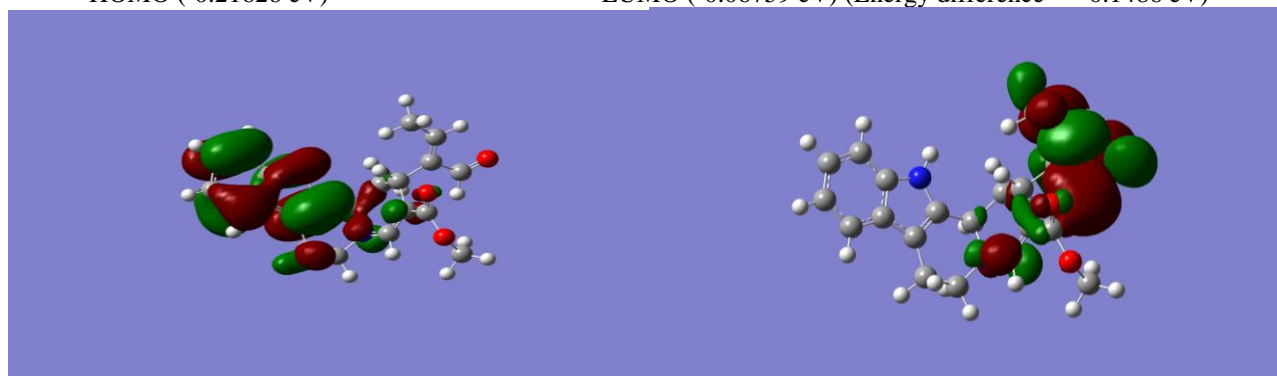


Figure 6 HOMO-LUMO plots for Iso-Vallesiachotamine obtained at B3LYP/6-31+G(d,p) level

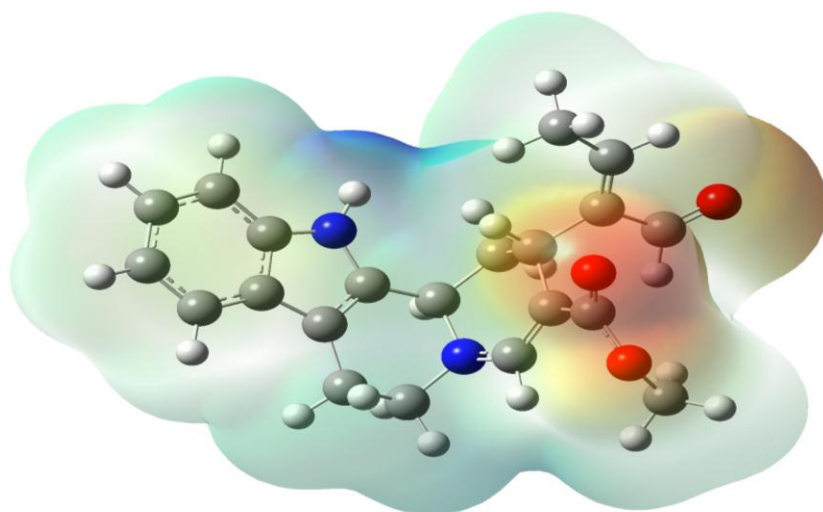


Figure 7 MESP plot for Iso-Vallesiachotamine obtained at B3LYP/6-31+G(d,p) level

Table 5: Intermolecular Energy and the Free energy of binding at a particular inhibition constant calculated by docking

S. No	Name of Protein Receptor	Intermolecular Energy (at Inhibition Constant)	Free Energy of Binding (at Inhibition Constant)
1	1GCN (Anti Diabetic)	-6.46 kcal/mol at 138.67 μ M	-5.26 kcal/mol at 138.67 μ M
2	2NMO (Pancreatic Cancer)	-7.57 kcal/mol at 21.29 μ M	-6.37 kcal/mol at 21.29 μ M
3	3I40 (Human Insulin)	-8.62 kcal/mol at 3.59 μ M	-7.43 kcal/mol at 3.59 μ M
4	1X2J (Lung Cancer)	-7.13 kcal/mol at 44.40 μ M	-5.94 kcal/mol at 44.40 μ M
5	5C5S (Several type Lung Cancer)	-7.10 kcal/mol at 47.18 μ M	-5.90 kcal/mol at 47.18 μ M

ACKNOWLEDGMENT

First author is thankful to the UGC, New Delhi for the financial assistance through the minor research project for carrying out the research work on the bioactive natural compounds at the place of his present affiliation. Authors are thankful to Prof. Neeraj Misra, Department of Physics, University of Lucknow, India for permitting us to access his computational facility. Thanks are due to Dr. D.P. Mishra and Dr. R.K. Maurya of C.D.R.I, Lucknow, India for providing the reports related to the various natural products. We are grateful to the Bioinformatics Resources & Applications Facility (BRAAF), C-DAC Pune, India, for providing us its supercomputing facility for performing quantum chemistry calculations. Thanks are due to Prof. Arthur J. Olson, department of Molecular Biology, Scripps Research Institute, La Jolla, USA for providing us the Auto Dock 4.2 Program for performing molecular docking study.

REFERENCES

- [1] D.P. Mishra, M.A. Khan, D.K. Yadav, A.K. Rawat, R.K. Singh, T. Ahamad, M.K. Hussain, M. Saquib, M.F. Khan, "Monoterpene Indole Alkaloids from *Anthocephalus cadamba* Fruits Exhibiting Anticancer Activity in Human Lung Cancer Cell Line H1299", Chemistry Select Vol.3, pp.8468-72, 2018. <https://doi.org/10.1002/slct.201801475>
- [2] D.P. Mishra, R. Maurya, "Isolation and Characterization of Bioactive Natural Products from Indian Medicinal Plants", PhD Thesis (Central Drug Research Institute, Lucknow, India) 2014.
- [3] E. Taşal, İ. Sıdır, Y. Gulseven, C. Öğretir, T. Onkol, "Vibrational spectra and molecular structure of 3-(piperidine-1-yl-methyl)-1,3-benzoxazol-2(3H)-one molecule by density functional theory and Hartree-Fock calculations". Journal of Molecular Structure Vol.923, pp.141, 2009.
- [4] A. Dwivedi, A.K. Srivastava, A. Bajpai, "Vibrational spectra, HOMO, LUMO, MESP surfaces and reactivity descriptors of amylamine and its isomers: A DFT study", Spectrochim Acta A Vol.149, pp.343 2015. <https://doi.org/10.1016/j.saa.2015.04.042>
- [5] A.K. Srivastava, A.K. Pandey, S. Jain, N. Misra, "FT-IR spectroscopy, intra-molecular C-H—O interactions, HOMO, LUMO, MESP analysis and biological activity of two natural products, triclisine and rufescine: FT and QAIM approaches", Spectrochim Acta A Vol.136, pp.682, 2015. doi: 10.1016/j.saa.2014.09.082.
- [6] A. Kumar, A.K. Srivastava, S. Gangwar, N. Misra, A. Mondal, G. Brahmachari, "Combined experimental (FT-IR, UV- visible spectra, NMR) and theoretical studies on the molecular structure, vibrational spectra, HOMO, LUMO, MESP surfaces, reactivity descriptor and molecular docking of Phomarin". J Mol Struct. Vol.1096, pp.94, 2015. <https://doi.org/10.1016/j.molstruc.2015.04.031>

- [7] L. Zhongqiang, Zhao-XuChen, J. Biaobing, "Density functional theory studies on the structures and vibrational spectroscopic characteristics of nickel, copper and zinc naphthalocyanines", *Spectrochimica Acta Part A: Molecular and Biomolecular Spectroscopy* Vol.217,pp.8-17,2019, <https://doi.org/10.1016/j.saa.2019.03.029>
- [8] S. Cosconati, S. Forli, A.L. Perryman, R. Harris, D.S. Goodsell, A.J. Olson, "Virtual screening with AutoDock: theory and practice". *Expert Opin. Drug Discovery* Vol.5,pp.597,2010, <https://doi.org/10.1517/17460441.2010.484460>
- [9] K. Sasaki, S. Dockerill, D.A. Adamiak, I.J. Tickle, T. Blundell, "X-ray analysis of glucagon and its relationship to receptor binding". *Nature* pp.257, 1975. <https://doi.org/10.1038/257751a0>
- [10] (a) B. Padmanabhan, K.I.Tong, Y.Nakamura, T. Ohta, M. Scharlock, "Structural basis for the defects of human lung cancer somatic mutations in the repression activity of *Keap1* on *Nrf2*". *RCSB PDB*, 2006. DOI: 10.2210/pdb1X2J/pdb (b) F.S.Yi, J.Q. Ren, W. Feng, "Crystal Structure of human Myosin 9b RhoGAP domain at 2.2 angstrom. *RCSB PDB*" 2015. DOI: 10.2210/pdb5C5S/pdb
- [11] D.Y. Oh, J.M. Oefsky, "G protien-coupled receptors as targets for anti-diabetic therapeutics", *Nat Rev Drug Discov.* Vol.5, pp.161, 2016. <https://doi.org/10.1038/nrd.2015.4>
- [12] P.C. Hawkins, A.G. Skillman, A. Nicholls, "Comparison of shape-matching and docking as virtual screening tools", *J Med Chem* Vol.50, pp.74, 2007. DOI: 10.1021/jm0603365
- [13] V.I. Timofeev, R.N. Chuprovetochin, V.R. Samigina, V.V. Bezuglov, K.A. Miroshnikov, I.P. Kuranova, "X-ray investigation of gene-engineered human insulin crystallized from a solution containing polysialic acid". *Acta Crystallogr Sect F Struct Biol Cryst Commun.* Vol.66(Pt-3)pp.259–263,2010. doi: 10.1107/S1744309110000461
- [14] Lucie Coppin, Audrey Vincent, Frédéric Frénois, Belinda Duchêne, Fatima Lahdaoui, "Galectin-3 is a non-classic RNA binding protein that stabilizes the mucin *MUC4mRNA* in the cytoplasm of cancer cells". *Scientific Reports* Vol.7, pp.43927, 2017. DOI: <https://doi.org/10.1038/srep43927>
- [15] A.D. Becke, "Density-functional thermochemistry. III. The role of exact exchange". *J. Chem. Phys.* Vol.98 pp.5648-5652, 1993. <https://doi.org/10.1063/1.464913>
- [16] C. Lee, W. Yang, R.G. Parr, "Development of the Colle-Salvetti correlation-energy formula into a functional of the electron density", *Phys. Rev. B* Vol.37, pp.785, 1988. DOI:<https://doi.org/10.1103/PhysRevB.37.785>
- [17] V. Barone, M. Cossi, "A new definition of cavities for the computation of solvation free energies by the polarizable continuum model". *J. Chem. Phys.* Vol.107, pp.3210, 1997. <https://doi.org/10.1063/1.474671>
- [18] M.J. Frisch, G.W. Trucks, H.B. Schlegel, G.E. Scuseria, M.A. Robb, J.R. Cheeseman G. Scalmani, V. Barone, B. Mennucci, G.A. Petersson, H. Nakatsuji, M.Caricato, X. Li, H.P. Hratchian, A.F. Izmaylov, J. Bloino, G. Zheng, J.L.Sonnenberg, M. Hada, M. Ehara, K. Toyota, R. Fukuda, J. Hasegawa, M. Ishida, T. Nakajima, Y. Honda, O. Kitao, H. Nakai, T. Vreven, Jr. J.A. Montgomery, J.E. Peralta, F. Ogliaro, M. Bearpark, J.J. Heyd, E. Brothers, K.N. Kudin, V.N.Staroverov, T. Keith, R. Kobayashi, J. Normand, K. Raghavachari, A. Rendell, J.C. Burant, S.S. Iyengar, J. Tomasi, M.Cossi, N. Rega, J.M. Millam, M. Klene, J.E. Knox, J.B. Cross, V. Bakken, C. Adamo, J. Jaramillo, R. Gomperts, R.E. Stratmann, O. Yazyev, A.J. Austin, R. Cammi, C. Pomelli, J.W. Ochterski, R.L. Martin, K. Morokuma, V.G. Zakrzewski, G.A. Voth, P. Salvador, J.J. Dannenberg, S. Dapprich, A.D. Daniels, O. Farkas, J.B. Foresman, J.V. Ortiz, J. Cioslowski and D.J. Fox, Gaussian 09, Revision B.01, Gaussian Inc. *J. Comput. Chem.* Vol.30 pp.2785, 2009.
- [19] G.M. Morris, R. Huey, W. Lindstrom, M.F. Sanner, R.K. Belew, D.S. Goodsell, A. J. Olson "Autodock4 and AutoDockTools4: automated docking with selective receptor flexibility". *J. Comput. Chem.*, Vol.30 pp.2785, 2009. DOI: 10.1002/jcc.21256
- [20] S. Forli, A.J. Olson, "A force field with discrete displaceable waters and desolvations entropy for hydrated ligand Docking". *J. Med. Chem.* Vol.55, pp.623, 2012. doi: 10.1021/jm2005145.
- [21] G.B. Ferreira, W.F. Azevedo, "Development of a machine-learning model to predict Gibbs free energy of binding for protein-ligand complexes". *Biophysical Chemistry* Vol.240,pp.63,2018. doi: 10.1016/j.bpc.2018.05.010.
- [22] (a)<https://www.rcsb.org/structure/1gcn>.DOI: 10.2210/pdb1Gcn/pdb (b)<https://www.rcsb.org/structure/1X2J>.DOI: 10.2210/pdb1X2J/pdb (c)<https://www.rcsb.org/structure/2NMO>.DOI: 10.2210/pdb2NMO/pdb (d)<https://www.rcsb.org/structure/3I4O>.DOI: 10.2210/pdb3I4O/pdb (e)<https://www.rcsb.org/structure/5C5S>. DOI: 10.2210/pdb5C5S/pdb
- [23] A.K. Mishra and S.P. Tewari, "DFT based modeling of a natural molecule-D-Myo-Inositol explores it to be a multifunctional biologically active" *AIP Conference Proceeding*, Vol.2100, 020067pp1-5, 2019. <https://doi.org/10.1063/1.5098621>
- [24] (a) R.M. Silversten, G.C. Bassler, Morrill, "Spectrometric Identification of Organic Compound", Jhon Wiley and sons 1991. (b) G. Socrates, "Infrared and Raman Characteristic group Frequencies", (3rd edn.) Wiley, New York 2001.
- [25] R. Dennington, T. Keith, J. Millam, Gauss View, Version 5, Semichem Inc., Shawnee Mission KS 2009.
- [26] J.P. Merrick, D. Morrann, L. Radom, "An Evaluation of Harmonic Vibrational Frequency Scale Factors". *J phys. chem. A* Vol.111, pp.11683, 2007. DOI: 10.1021/jp073974n
- [27] T. Schlick, "Molecular Modeling and Simulation: An Interdisciplinary Guide" (2nd edn.), Springer, New York Vol. 21, 2010. DOI 10.1007/978-1-4419-6351-2 1
- [28] R.G. Pearson, "Absolute electronegativity and hardness correlated with molecular orbital theory", *proc. Natl. Acad. Sci. (USA)* Vol.83 pp.8440, 1986. PMID: 16578791
- [29] (a) M. Belletete, J.F. Morin, M. Leclerc, G. Durocher, "A theoretical, spectroscopic, and photophysical study of 2, 7-carbazolenevinylene-based conjugated derivatives". *J.Phys. Chem. A* 109 (2005) 6953, DOI: 10.1021/jp051349h (b) D. Zhenminga, S. Heping, L. Yufang, L. Diansheng, L. BoL, "Experimental and theoretical study of 10-methoxy-2-phenylbenzo[h]quinoline". *Spectrochimica. Acta Part A* Vol.78, pp.1143, 2011. <https://doi.org/10.1016/j.saa.2010.12.067>
- [30] D.F. Lewis, C. Loannides, D.V. Parke, "Interaction of a series of nitriles with the alcohol-inducible isoform of P450: computer analysis of structure-activity relationships". *Xenobiotica* Vol.24,pp.401,1994 <https://www.ncbi.nlm.nih.gov/pubmed/8079499>
- [31] (a) E. Scrocco, J. Tomasi, "Reactivity and Intermolecular Forces: An Euristic Interpretation by Means of Electrostatic Molecular Potentials". *Adv. Quantum Chem.* Vol.11,pp.115,1978. [https://doi.org/10.1016/S0065-3276\(08\)60236-1](https://doi.org/10.1016/S0065-3276(08)60236-1) (b) F.J. Luque, J.M. Lopez, M. Orozco, "Electrostatic interactions of a solute with a continuum. A direct utilization of ab initio molecular potentials for the prevision of

- solvent effects*". Perspective on Theor. Chem. Acc. Vol.10, pp.343, 2000. https://doi.org/10.1007/978-3-662-10421-7_56
- [32] (a) E. Scrocco, J. Tomasi, "Topics in Current Chemistry" Vol.7, pp.95, 1973. <https://www.springer.com/series/128> (b) Y. Li, Y. Liu, H. Wang, X. Xiong, P. Wei, F. Li, "Synthesis, Crystal Structure, Vibration Spectral, and DFT Studies of 4-Aminoantipyrine and Its Derivatives". *Molecules* Vol.18, pp. 877, 2013. <https://doi.org/10.3390/molecules18010877>
- [33] M. Arirazhagan, J. K. Senthil, "Vibrational analysis of 4-amino pyrazolo (3,4-d) pyrimidine A joint FTIR, Laser Raman and scaled quantum mechanical studie". *Spectrochim. Acta, Part A* Vol.82, pp. 228, 2011. <https://doi.org/10.1016/j.saa.2011.07.040>
- [34] V. Arjunan, S. Thillai Govindaraya, P. Ravindran, S. Mohan, "Exploring the structure-activity relations of N-carbathoxyphthalimide by combining FTIR, FT-Raman and NMR spectroscopy with DFT electronic structure method. *Spectrochim*". *Acta Part A* Vol.120, pp. 473, 2014. DOI: 10.1016/j.saa.2013.10.025
- [35] N. Sundaraganesan, S. Ilakiamani, B.D. Joshua, "FT-Raman and FT-IR spectra, ab initio and density functional studies of 2-amino-4, 5-difluorobenzoic acid". *Spectrochim. Acta Part A*, Vol.67, pp. 287, 2007. <https://doi.org/10.1016/j.saa.2006.07.016>

AUTHORS PROFILE

Dr. Ashok Kumar Mishra pursued B.Sc. (Physics & Mathematics), M.Sc. (Physics) and Ph.D. (Physics) from DDU Gorakhpur University, Gorakhpur, Uttar Pradesh, India in 1996, 1998 & 2006 respectively. He also qualified National Eligibility Test (NET) in Physical Sciences in 2002. He was appointed as Lecturer, Physics in

Amity University Uttar Pradesh, Lucknow Campus, India in September 2004 and continued working there till June 2015. He is currently working as Assistant Professor, Department of Physics in Dr. Shakuntala Misra National Rehabilitation University, Lucknow, India since June 2015. He is Life member of Materials Research Society of India (MRSI) since 2008 and a life member of the Indian Science Congress Association (ISCA) since 2013. He has published more than 30 research papers in reputed international journals including SCOPUS indexed, Thomson Reuters (SCI & Web of Science) and conferences including IEEE and it is also available online. He has one published patent and authorship of 02 books to his credit. His main research work focuses on Organic semiconductors, Biosensors, Bio molecules, Chemical Physics and Atomic & Molecular Physics. He has 15 years of simultaneous teaching and research experience at University level.

Mr. Satya Prakash Tewari pursued B.Sc. (Physics & Mathematics), M.Sc.(Physics) from RML Avadh University, Ayodhya, Uttar Pradesh, India in 2007 and 2009 respectively. He is currently pursuing Ph.D. in Physics under the supervision of Dr. Ashok Kumar Mishra, Assistant Professor, Department of Physics in Dr. Shakuntala Misra National Rehabilitation University, Lucknow, India since August 2016. He has published 04 research papers in reputed international journals including SCOPUS indexed, Thomson Reuters (SCI & Web of Science) and conferences and it's also available online. His main research work focuses on the Bio molecules.
